

Article

Burning Characteristics of Ancient Wood from Traditional Buildings in Shanxi Province, China

Yufei Wang¹, Weibin Wang², Haibin Zhou^{1,*}  and Fei Qi³¹ Research Institute of Wood Industry, Chinese Academy of Forestry, Beijing 100091, China; wyfjch@163.com² Shanxi Academy of Ancient Building, Sculpture and Mural Protection, Taiyuan 030012, China; sxwj1528@163.com³ The Palace Museum, Beijing 100009, China; qfei87@126.com

* Correspondence: zhouhb@caf.ac.cn; Tel.: +86-18610686972

Abstract: Due to long-term natural degradation, the surface morphology of traditional building wood differs significantly from that of modern wood. It is more combustible than modern wood and its combustion characteristics are important evaluation indicators for fire simulation and fire protection of traditional buildings. In this paper, ancient wood from six traditional buildings were tested by a surface morphology fractal method and conical calorimeter. Additionally, their combustion properties such as ignition time, heat release rate, total heat release and charring time were analyzed to determine the combustion behavior of ancient wood and their differences with modern wood. The results showed that the ignition time of the specimens was significantly influenced by the surface morphological features. The higher the fractal dimension grade of the morphological features, the shorter the ignition time. The ignition time of Ulm wood with fractal dimension class 3 was 15 s, while that of Ulm wood with fractal dimension class 1 was 23 s. Under the same fractal dimension class, the total heat release per unit time of ancient softwood was higher than that of ancient hardwood. The average heat release rates of Larch wood and Ulm wood were $66.21 \text{ kw}\cdot\text{m}^{-2}$, $72.07 \text{ kw}\cdot\text{m}^{-2}$ and $57.26 \text{ kw}\cdot\text{m}^{-2}$, $67.30 \text{ kw}\cdot\text{m}^{-2}$. The basic charring rate of ancient wood of the same species was mostly higher than that of modern wood by more than 6%, with the basic charring rate of ancient Larch wood being $0.8559 \text{ mm}/\text{min}$, which was 15.66% higher than that of modern Larch wood, 22.27% higher than that recommended in the European EC5 standard, and 6.87% higher than that calculated in the American AFPA. The results of the study are important guidelines for fire risk assessment and fire protection of traditional buildings.

Keywords: traditional buildings; ancient wood; combustion properties; cone calorimetry

Citation: Wang, Y.; Wang, W.; Zhou, H.; Qi, F. Burning Characteristics of Ancient Wood from Traditional Buildings in Shanxi Province, China. *Forests* **2022**, *13*, 190. <https://doi.org/10.3390/f13020190>

Academic Editor: Sofia Knapić

Received: 21 December 2021

Accepted: 20 January 2022

Published: 26 January 2022

Publisher's Note: MDPI stays neutral with regard to jurisdictional claims in published maps and institutional affiliations.



Copyright: © 2022 by the authors. Licensee MDPI, Basel, Switzerland. This article is an open access article distributed under the terms and conditions of the Creative Commons Attribution (CC BY) license (<https://creativecommons.org/licenses/by/4.0/>).

1. Introduction

Wood is often used as the main material in traditional buildings, which is highly combustible compared to other modern building materials. Traditional buildings have important historical and artistic values and are not renewable. In the event of a fire, irreparable damage will be caused. In recent years, fires in traditional buildings have often occurred. On 3 January 2015, Gongchen Building, an ancient city in Yunnan, China with a history of more than 600 years, was reduced to rubble in a fire that largely destroyed the wooden parts. The fire area reached 765 square meters. On 2 September 2018, the National Museum of Brazil went up in flames, the fire burning for six hours, destroying all the roof beams. On 15 April 2019, a fire broke out at Notre Dame de Paris in the French capital, starting in the attic and then spreading to the entire roof, before eventually collapsing at the spire. Its postdisaster reconstruction is affected by the stability of the remaining masonry structures [1]. On 31 October 2019, a fire broke out in Shurijo Castle, Okinawa Prefecture, Japan, destroying the main hall and an adjacent traditional building and making it difficult to control the fire. On 4 May 2020, a fire broke out in Yongjia Sima Di's house, covering

an area of 1246 square meters and destroying more than half of the traditional building complex. As of last year, the total number of major historical and cultural sites protected at the national level in China reached 5058, with Shanxi Province ranking first with a total of 530, accounting for 10.4% of the total number of sites. China's existing state-protected units have the most traditional buildings, with a total of 2162, accounting for 42.7% of them all. Shanxi Province currently has 18,118 traditional buildings with wooden structures, and 72.6% of the wooden buildings are built before the Song Dynasty and the Yuan dynasty, of which 119 are major historical and cultural sites protected at the national level. The fire at the Wu Temple on 30 May 2019 was the most serious traditional building fire in Shanxi Province in recent years. Located on Shuyuan Street in the ancient city of Pingyao, Shanxi Province, China, the Wumiao Temple covers a total area of about 4360 square meters. It was built in the Qing Dynasty. The fire had an overfire area of about 50 square meters and caused the main building of the Wu Temple to burn down and collapse.

Wood is a flammable material. For the study of its combustion performance, conical calorimeter experiments, thermogravimetric analysis and differential thermal analysis are mainly used to analyze the heat release rate, mass loss, specific extinction area and the variation law of gas yield such as carbon monoxide to deduce the combustion process of wood and even wood-frame buildings [2]. Ji, J. [3] analyzed the parameters of wood ignition time and ignition temperature under different ranges of radiant heat flow, and summarized the changes in mass loss, surface and internal temperatures of wood under nonconstant heat radiation with time. They concluded that with the increase in radiant heat flow, the ignition time shortens and the ignition temperature decreases, the mass loss rises and the rate of smoke production increases, which provides some guidance for fire rescue. Beaumon et al. [4] studied the effect of pyrolysis parameters such as temperature, heating rate, and grain size on the wood pyrolysis process. Kanury and Blackshear [5] investigated various physicochemical effects during charring, including inward diffusion of condensable vapors, outward diffusion of internal convection, the nature of partially charred wood, pyrolysis kinetics, pyrolysis energetics, and posted composition reactions. From a wood science perspective, the species, microstructure, chemical composition, and some of the physical properties of wood affect charring. Maraveas et al. [6] also obtained a correlation between density and charring in experiments with 13 kinds of hardwood and two kinds of softwood. In comparison to hardwood, most of softwood have a lower density, while hardwood have better thermal conductivity, and are more difficult to precipitate combustion and flammable volatile fractions. The relative charring rate is slower than that of softwood; Tomassetti, M. et al. [7] used thermogravimetric analysis to analyze the main chemical composition and the amount remaining after degradation of modern and ancient wood in an old church porch, and confirmed the relationship between lignin and cellulose content and the age of the wood samples. Wang [8] used thermogravimetric analysis and characteristics experiments to study the aging degree of ancient pine and the change pattern of combustion characteristics. The ignition point of ancient pine was found to be 19.83 °C lower than that of modern pine. Additionally, the charred layer of ancient pine is more sparse, which also leads to the ignition time and peak time of ancient pine wood being lower than modern pine. Weng, Janssens and Li et al. [9–11] measured wood under constant external thermal radiation by means of thermocouples and other methods. The surface temperature of wood during ignition was measured by thermocouples and other methods under constant external heat radiation, and the surface ignition temperature of wood was in the range of about 200–540 °C. Ji [12] measured the ignition time of four woods, namely, white flowered paulownia, elm, red toon and acacia, by adjusting the heat radiation plate to simulate the different heat radiation intensity of the materials in a real fire environment, and proposed the basis for judging wood ignition: wood was ignited when its surface temperature reached 500 °C and the rate of change of heat flow was greater than 0.07 kW/(m²·s). Xiang [13] used thermogravimetric analysis to characterize the pyrolysis kinetics characteristics of pinus koraiensis, hemlock and spruce from the Potala Palace in Lhasa, China. Among the three woods, pinus koraiensis was the most difficult to degrade,

while spruce was the most easily degraded. Compared to other building materials, wood is extremely flammable. So, it is very important to fireproof traditional buildings.

The nonrenewable nature and inheritance of traditional buildings make them of great spiritual and cultural value, and they are the precious cultural heritage left to us by history. However, because the heritage buildings have experienced hundreds or even thousands of years of ultraviolet radiation, rain and snow, as well as long periods of natural drying, surface decay, cracks and holes are very common [14]. The wood surface density decreases, forming a unique degraded form, increasing the air contact area. The overall building fire load is abruptly increased. In terms of fire prevention and control, the current approach is to prevent fires, build models to simulate fire scenes, identify weak points in fire protection, and prevent fires before they occur. Frangi and Fontana [15–18] conducted a systematic study of wood fire resistance and wood-structure fire protection, including studies of the fire safety of multistorey wood-frame houses, the charring rate and cross-sectional temperature distribution of wood, cavity charring model and design of wood panels, fire resistance of glued, laminated timber beams, and fire resistance of wood structures with protective layers. Frangi A, Knobloch M and Fontana M [19] conducted fire resistance tests on cross-laminated timber floor slabs and concluded that the fire resistance duration of the panels treated against fire was significantly higher than that of the untreated panels. Bai [20] established an FDS fire model for wooden traditional buildings with different fire sources and monitoring points, which can simulate the fire scene to some extent, but the accuracy of the model is limited by the number of software grids as well as boundary conditions. Gao [21] also used the FDS software to establish a fire spread model for wood structure fires with different fire sources at different locations with characteristics of typical wood structure dwellings in Lijiang, and gave a safe fire distance applicable to local wood structure buildings in Lijiang, which provides a basis for the hazard assessment of local wood-structure engineering projects. From previous studies we can also see that most of the fire resistance tests as well as fire simulation tests used modern wood, but its performance differs from ancient wood. Substituting the combustion characteristics of modern wood into the traditional building fire model is questionable. Modern wood parameters are also limited in their guidance for predicting the overall fire load rating and deployment of fire safety facilities in traditional buildings.

In this thesis, by selecting ancient wood replaced by maintenance of representative heritage buildings in Shanxi Province, the ignition time, heat release rate, total heat release and charring time of different species of wood with different surface morphology were examined to obtain some deterministic raw data. And analyze the difference of combustion characteristics between ancient wood and modern wood, to provide more accurate data support for fire retarding of ancient wood and firefighting of heritage buildings.

2. Materials and Methods

2.1. Materials

As shown in Table 1 and Figure 1, different surface morphologies of ancient wood were sampled by a uniform, standard photographic method. Fractal dimension analysis was applied to Matlab to classify the surface morphology of ancient wood into three classes. According to this basis, divided into levels 1, 2, and 3, grade 1 fractal dimension interval is less than 1.4, and means there is less surface cracking or the overall shape of the wood is more uniform; grade 2 fractal dimension interval is 1.4–1.6, and the surface shape has obvious cracking or parts of the surface have uneven wood; grade 3 fractal dimension interval is greater than 1.6, and the surface is obviously uneven or there is a high degree of deterioration of the wood.

Table 1. Sample Information.

Number	Traditional Building	Member Name	Wood Species	Year of Construction	Sample Name	Pictures
1	Baitai Temple(Xinjiang, Yuncheng)	column	Ulm wood (<i>Ulmus</i> spp.)	The Tang Dynasty	A1 A2 A3	
2	Wenmiao Temple(Daixian, Xinzhou)	column	Larch wood (<i>Larix</i> spp.)	Built in Tang Dynasty, restored in Yuan Dynasty	B1 B2 B3	
3	Tudimiao Temple(Yangcheng, Jincheng)	beam	Salix wood (<i>Salix</i> spp.)	The Ming Dynasty	C3	
4	Baiyu Palace(Lingchuan, Jincheng)	column	Poplar wood (<i>Populus</i> spp.)	Before the Jin Dynasty	D1	
5	Dongyue Temple(Runcheng, Yangcheng)	column	Ailanthus wood (<i>Ailanthus</i> spp.)	Before the Jin Dynasty	E1 E2	
6	Jinci Temple (Taiyuan)	column	Larch wood (<i>Larix</i> spp.)	The Yuan Dynasty	F1	



Figure 1. Sample pictures: (A1) Ulm wood, fractal dimension 1.3536, grade 1, Baitai Temple, (A2) Ulm wood, fractal dimension 1.4250, grade 2, Baitai Temple, (A3) Ulm wood, fractal dimension 1.6211, grade 3, Baitai Temple, (B1) Larch wood, fractal dimension 1.2656, grade 1, Wenmiao Temple, (B2) Larch wood, fractal dimension 1.5766, grade 2, Wenmiao Temple, (B3) Larch wood, fractal dimension 1.6786, grade 3, Wenmiao Temple, (C3) Salix wood, fractal dimension 1.7342, grade 3, Tudimiao Temple, (D1) Poplar wood, fractal dimension 1.2400, grade 1, Baiyu Palace, (E1) Ailanthus wood, fractal dimension 1.0575, grade 1, Dongyue Temple, (E2) Ailanthus wood, fractal dimension 1.5393, grade 2, Dongyue Temple, (F1) Larch wood, fractal dimension 1.3045, grade 1, Jinci Temple.

The test intercepted the outermost layer of wood containing the surface form at a depth of 50 mm. The specimen size was cut to 100 mm × 100 mm × 40 (±5) mm (L × R × T) while retaining the surface form. Before testing, the moisture content of the specimen was adjusted to 12% at a temperature of 20 ± 2 °C and a relative humidity of 65 ± 3%.

The specimen numbers are shown in the following table, Group A is the back eaves of the Baitai Temple(Xinjiang, Yuncheng), built in the 14th year of the Kaiyuan era of the Tang Dynasty, made of Ulm wood, and three specimens are taken according to the fractal dimension grade, A1 is 1.3536, A2 is 1.4250, A3 is 1.6211. Group B is the eaves of the main hall of the Wenmiao Temple(Daixian, Xinzhou), built in the Tang Dynasty, made of Larch wood, and three specimens are taken according to the fractal dimension grade, B1 is 1.2656, B2 is 1.5766, B3 is 1.6786. Group C is the beams of the Tudimiao Temple(Yangcheng, Jincheng), built in the Ming Dynasty, made of Salix wood, where the overall deterioration of the surface tends to be the same, and one specimen is taken according to the fractal dimension class and recorded as C3. Group D is the column of the middle hall of the Baiyu Palace(Lingchuan, Jincheng), built before the Jin Dynasty, made of poplar wood, and one specimen is taken according to the fractal dimension class and recorded as D1. Group E is the column of Dongyang Temple(Runcheng, Yangcheng), which was built before the Jin Dynasty, made of Ailanthus wood, and two specimens are taken according to the fractal dimension grade, E1 is 1.0575, E2 is 1.5393. Group F is the column of Jinci Temple(Taiyuan), built in the Yuan Dynasty, made of Larch wood, and one specimen is taken as F1 according to the fractal dimension class.

The density of the specimen is shown in Table 2. Samples were taken from the more structurally sound part of the experimental material. Determine the basic density($\text{g}\cdot\text{cm}^{-3}$) of the specimen according to GB/1933-2009 Method for determination of the density of wood. The data is provided here as a record of the material.

Table 2. Density of the specimen.

Sample Name	Density ($\text{g}\cdot\text{cm}^{-3}$)	
	Mean Value	COV(%)
A1	0.592	4.22
A2	0.580	3.70
A3	0.523	3.02
B1	0.429	6.19
B2	0.405	5.66
B3	0.404	3.26
C3	0.522	3.32
D1	0.372	3.76
E1	0.510	4.63
E2	0.498	4.33
F1	0.461	5.08

2.2. Test Methods

2.2.1. Combustion Performance Test

In this study, five combustion performance parameters were tested for evaluation: time to ignition (TTI), heat release rate (HRR), total heat release (THR), mass of combustion residue, mass of material remaining after combustion, and charring time. The burning properties of ancient wood were tested with reference to the ISO 5660-1 standard [22]. The use of conical calorimeter tests provides an accurate and comprehensive understanding of the changes in multiple combustion parameters of wood during the whole process from ignition to extinction under a constant applied heat source, and can provide more accurate parameters for fire simulation. To ensure thermal boundary conditions on the back of the sample, five faces of the sample were wrapped in aluminum foil and placed in the combustion rack. The external heat flux was $35 \text{ kW}\cdot\text{m}^{-2}$. The instrument automatically reads the data every 1s and stores and calculates it.

We intercepted the areas of wood surface with different fractal dimension classes. For example, one specimen was labeled A1, where A represents the source of the specimen, the back eaves column of the White Terrace Temple in Xinjiang County, made of Ulm wood, and 1 represents that its surface fractal dimension is in the interval of grade 1. The specimens are intercepted, and the specimen size is 100 mm × 100 mm × 40 (±5) mm (L × R × T), retaining the outermost surface morphology of the sample, such as cracks, decay, wear, etc. The highest individual sample surface thickness does not exceed 45 mm.

2.2.2. Charring Rate Test

As shown in Figure 2, cavities were drilled in the middle of the combustion surface at 10 mm, 20 mm and 30 mm in the thickness direction and a temperature measuring resistor wire was placed. The resistance wire is connected to a real-time temperature monitor and the real-time temperature is collected and recorded every 5 s.

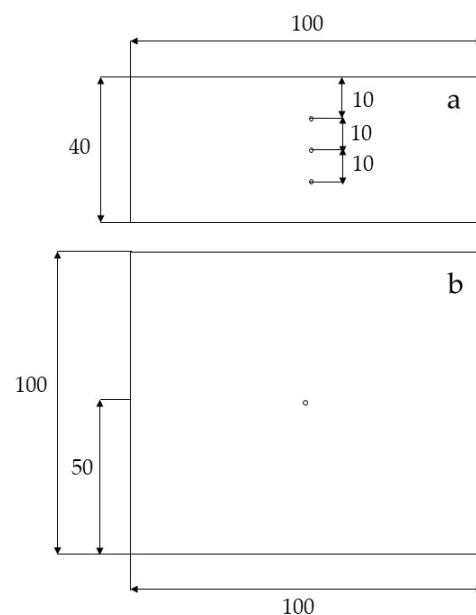


Figure 2. Thermocouple placement and depth (unit: mm). (a): side view; (b): plan view.

At present, the charring limit temperature of wood varies from region to region, such as 260 °C, 288 °C and 300 °C. The charring rate of wood with 260 °C and 288 °C as the charring limit temperature is relatively conservative in terms of fire protection design, and the cross-section of members is larger under the same conditions. Furthermore, 300 °C as the charring limit temperature is increasingly accepted by many scholars [23]. In this experiment, 300 °C was used as the charring limit temperature. The three resistance wires of different thicknesses were recorded when they reached 300 °C. The experiment was stopped when the temperature of the resistance wire at the farthest end from the fire surface reached 300 °C. If the slope of the heat release rate curve decreased with a gentle trend when the temperature of the lowest end reached 300 °C, the experiment was continued until the second peak of the heat release rate appeared, and if the heat release rate curve had been in a rising state, the experiment was stopped according to the regulations.

The instantaneous charring rate is calculated as follows:

$$\beta_i = \frac{d_i}{t_i}, \quad i = 1, 2, 3$$

where: β_i —instantaneous charring rate (mm/min); d_i —height of the temperature resistance wire from the upper surface of the specimen (mm); t_i —time for the temperature resistance wire to reach 300 °C. A linear relationship between d_i and t_i is established and the slope of the linear regression is defined as the basic charring rate.

The basic charring rate of ancient wood measured in this experiment was compared with the charring rate design values recommended by the European EC5 standard, the Canadian Code, the Australian Code and the American AFPA [24–26]. The basic charring rate is 0.5 mm/min for hardwood and 0.7 mm/min for softwood in the European EC5 standard, and the design value for charring rate is 0.6 mm/min in the Canadian code. The Australian code specifies the charring rate as a function of wood density ρ : $\beta = 0.4 + (280/\rho)^2$. The calculation method recommended by the American AFPA uses the effective charring rate, taking into account the rounding effect at the edges of the member and the reduction in strength and stiffness of the wood heated within the charring line:

$$\beta_{\text{eff}} = 1.2 \beta_n / t^{0.187}$$

where: β_n is the nominal charring rate, taken as 0.635 mm/min; t is the fire time (h).

3. Results

3.1. Ignition Time

The combustion properties of wood specimens are shown in Table 3. The time to ignition (TTI) is the most important characteristic of combustible materials from the standpoint of fire prevention. It is the time used from the time the surface of the material is heated to the time when the surface continues to appear to burn at a predetermined intensity of incident heat flow, and can be used to evaluate and compare the fire resistance of materials. The longer the ignition time, the better the fire resistance of the material. Extending the ignition time of wood is an important aspect of fire resistance of wood materials.

Table 3. Combustion performances of different specimens.

Material		Ignition Time TTI/s	Heat Release Rate HRR (kw·m ⁻²)		Total Heat Release THR (MJ·m ⁻²)	Mass Loss (g)
			Average Mean HRR	Peak/Time Peak HRR		
Ulm wood	A1	23	57.26	126.60/50	102.78	109.03
	A2	20	63.70	116.66/45	114.65	135.91
	A3	15	67.30	166.84/35	121.14	149.97
Larch wood	B1	15	66.21	149.21/30	118.18	81.90
	B2	11	70.68	141.24/30	126.22	77.19
	B3	11	72.07	141.27/30	128.70	88.91
Salix wood	F1	16	61.64	116.01/30	110.72	78.75
	C3	17	72.35	144.94/20	129.79	95.15
Poplar wood	D1	7	62.46	142.97/30	111.19	76.27
Ailanthus wood	E1	30	64.37	92.95/45	115.87	100.73
	E2	14	64.90	110.00/30	115.86	78.52

From Table 3, it can be seen that the ignition time of ancient construction wood is closely related to the surface fractal dimension, and the higher the fractal dimension grade, the shorter the ignition time. The ignition time of Ulm wood with fractal dimension grade 3 is 15 s, which is 8 s shorter than that of Ulm wood with fractal dimension grade 1. The ignition time of Ailanthus wood with fractal dimension grade 2 is 14 s, which is 16 s shorter than that of Ailanthus wood with fractal dimension grade 1. The ignition time of hardwood in ancient wood is essentially longer than that of softwood, among which the ignition time of Ailanthus wood E1 is the longest, reaching 30 s, and that of poplar wood is the shortest, 7 s. The ignition time was the shortest at 7 s.

3.2. Heat Release Rate

Figure 3 shows the results of heat release rate tests for ancient wood. Figure 3a shows the real-time heat release rate curves for three fractal dimension classes of Ulm, Figure 3b shows the real-time heat release rate curves for three fractal dimension classes of Larch

wood, Figure 3c shows the real-time heat release rate curves for five specimens with fractal dimension class 1, Figure 3d shows the real-time heat release rate curves for three specimens with fractal dimension class 2, and Figure 3e shows the real-time heat release rate curves for three specimens with fractal dimension class 3.

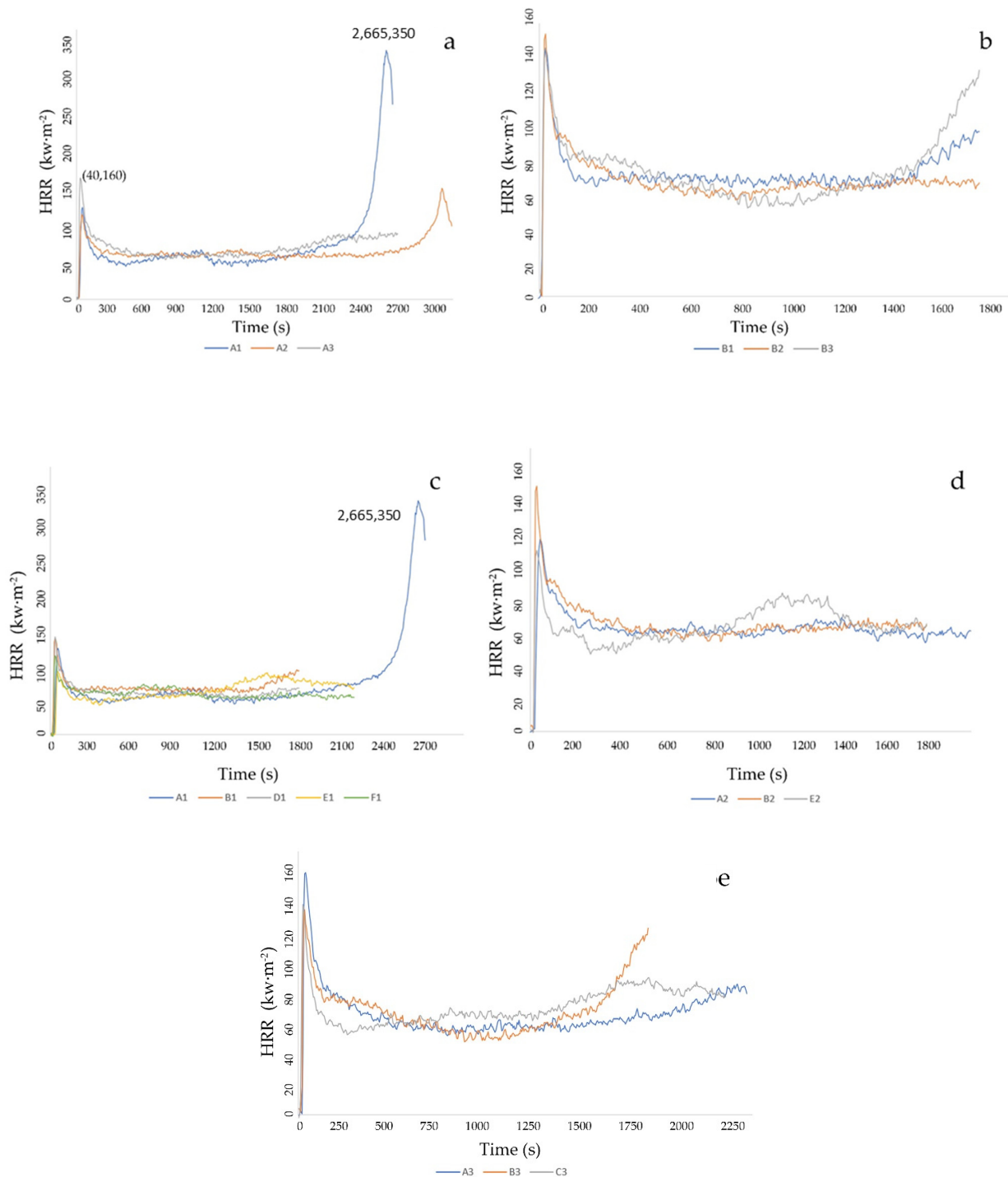


Figure 3. Heat release rate of ancient wood with different fractal dimension classes: (a) heat release rate curves for three fractal dimension classes of Ulm, (b) heat release rate curves for three fractal dimension classes of Larch wood, (c) heat release rate curves for five specimens with fractal dimension class 1, (d) heat release rate curves for three specimens with fractal dimension class 2, (e) heat release rate curves for three specimens with fractal dimension class 3.

From the point of view of fire development after a material has been ignited, the heat release rate is the dominant influence and is an important performance parameter used to characterize fire strength. The peak heat release rate (peak HRR) represents the maximum degree of heat release from the burning of a material. The greater the value of both, the greater the heat release from combustion of the material and the higher the fire hazard posed. From Figure 3a, it can be seen that the heat release rate curve of Ulm in hardwood shows a bimodal shape, and the first peak is the wood surface decomposition due to flaming combustion, releasing a large amount of heat, so that the heat release rate reaches the first peak of $160 \text{ kw}\cdot\text{m}^{-2}$. Then, the pyrolysis of wood begins to move from the surface to the interior, gradually forming a charred layer, making the overall trend after the first peak begin to decline, with the stabilization of pyrolysis. The release rate gradually stabilizes, forming a flat phase in the middle of the figure. When the thermal interface reaches the back of the specimen, the charred layer is destroyed and the heat release rate begins to rise to reach a second peak of $350 \text{ kw}\cdot\text{m}^{-2}$, followed by a gradual shift of pyrolysis to charred residue negative combustion and a gradual decrease in the heat release rate. The rest of the species had only the first peak, and the maximum value did not exceed $150 \text{ kw}\cdot\text{m}^{-2}$. Larch wood, Salix wood, Poplar wood and Ailanthus wood already showed upwards and downwards fluctuations of unstable heat release rates in the otherwise gentle charring layer stage, and their charring layers were not well-protected.

For the same fractal dimension class, the total heat release per unit time was higher for ancient softwood than for ancient hardwood, with average heat release rates of $66.21 \text{ kw}\cdot\text{m}^{-2}$, $72.07 \text{ kw}\cdot\text{m}^{-2}$ and $57.26 \text{ kw}\cdot\text{m}^{-2}$, $67.30 \text{ kw}\cdot\text{m}^{-2}$ for Larch wood and Ulm wood at fractal dimension classes 1 and 3, respectively. The higher the fractal dimension class of the same species, the higher the average heat release rate.

3.3. Total Heat Release

Figure 4 shows the results of the total real-time heat release tests for the ancient wood. Figure 4a shows the total real-time heat release curves for three fractal dimension classes of Ulm, Figure 4b shows the total real-time heat release curves for three fractal dimension classes of Larch wood, Figure 4c shows the total real-time heat release curves for five specimens with fractal dimension class 1, Figure 4d shows the total real-time heat release curves for three specimens with fractal dimension class 2, and Figure 4e shows the real-time total heat release curves for three specimens with fractal dimension class 3.

Total heat release (THR) is the sum of the heat released from ignition to flame extinction dimension of a material at a set intensity of incident heat flow, and can be considered in conjunction with heat release rate to better evaluate the flammability and fire resistance of a material. The greater the total heat release, the more combustible the material is and the higher the fire hazard. As can be seen in Figure 4, the total heat release of hardwood and softwood is similar in the same burning time and the overall trend is the same, but the total heat release of Ulm reaches $180 \text{ MJ}\cdot\text{m}^{-2}$, indicating that the heat resistance of softwood is stronger than that of hardwood. However, the slope of the total heat release curve of ancient wood, whether hardwood or softwood, is basically smooth, or even shows an increasing trend. Unlike the trend in modern wood that produce a flat phase after the flaming stage, the total heat release curve of ancient wood shows a continuous high growth rate, the total heat release increases, and the danger of fire is high.

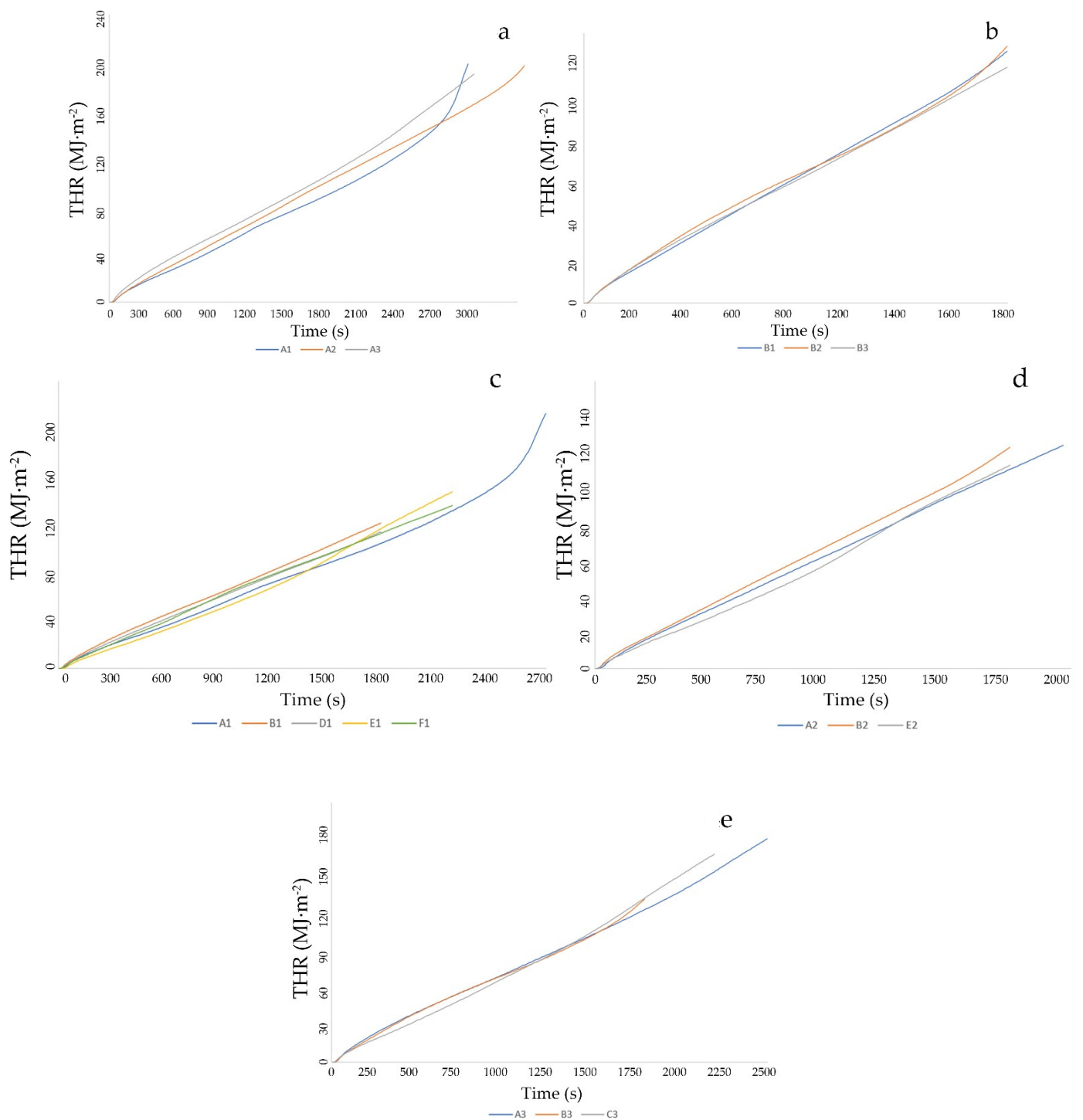


Figure 4. Total heat release of ancient wood with different fractal dimension classes: (a) THR of three fractal dimension classes of Ulm, (b) THR of three fractal dimension classes of Larch wood, (c) THR of five specimens with fractal dimension class 1, (d) THR of three specimens with fractal dimension class 2, (e) THR of three specimens with fractal dimension class 3.

3.4. Charring Rate

The time and instantaneous charring rates calculated for the three different locations of the specimens when the temperature resistance reached 300 °C are shown in Table 4, and the basic charring rates of the specimens are shown in Table 5. The basic charring rates

of the wood compared to modern wood and the standard recommended values are shown in Table 6 [27–30].

Table 4. Instantaneous charring rates of samples.

Species	t1 (min)	t2 (min)	t3 (min)	β_1 (mm/min)	β_2 (mm/min)	β_3 (mm/min)
A1	12.25	29.50	53.42	0.8163	0.6779	0.5616
A2	11.75	32.92	53.08	0.8511	0.6075	0.5651
A3	11.27	25.18	41.02	0.8873	0.7943	0.7314
B1	4.67	13.58	27.65	2.1413	1.4728	1.0850
B2	6.60	16.48	24.87	1.5151	1.2136	1.2063
B3	5.14	10.78	22.93	1.9455	1.8553	1.3082
C3	12.28	23.35	35.28	0.8143	0.8565	0.8503
D1	8.40	16.68	26.15	1.1905	1.1990	1.1472
E1	4.92	22.30	33.58	2.0325	0.8968	0.8934
E2	6.55	15.33	26.75	1.5267	1.3046	1.1215
F1	11.52	21.15	35.58	0.8681	0.9456	0.8432

Table 5. Basic charring rates of samples.

Species	Charring Rate (mm/min)	R ²	
Softwood	B1	0.8559	0.9835
	B2	1.0923	0.9978
	B3	1.0762	0.9986
	D1	1.1251	0.9985
	F1	0.8204	0.9869
Hardwood	A1	0.4816	0.9913
	A2	0.4838	0.9998
	A3	0.6713	0.9986
	C3	0.8692	0.9995
	E1	0.6875	0.9851
	E2	0.9845	0.9943

Table 6. Basic charring rates and standard recommended values for ancient and modern wood.

Species	β_1 (mm/min)	β_2 (mm/min)	β_3 (mm/min)	Charring Rate (mm/min)	
Larch wood	Ancient wood	2.1413	1.4728	1.0850	0.8559
	Modern wood	0.72	0.64	0.68	0.74
	EC5	-	-	-	0.7
	NBCC2010	-	-	-	0.6
	AS1720.4	-	-	-	0.84
	AFFA	-	-	-	0.8009
Poplar wood	Ancient wood	1.1905	1.1990	1.1472	1.1251
	Modern wood	0.95	0.85	0.95	0.95
	EC5	-	-	-	0.7
	NBCC2010	-	-	-	0.6
	AS1720.4	-	-	-	0.8489
	AFFA	-	-	-	0.8900

The basic charring rate of ancient wood of the same species was mostly higher than that of modern wood by more than 5%, in which the basic charring rate of ancient Larch wood was 0.8559 mm/min, which was 15.66% higher than that of modern Larch wood, 22.27% higher than the recommended value in the European EC5 standard, 1.89% higher than the calculated value in the Australian code, and 6.87% higher than the calculated value in the American AFFA. The basic charring rate of Larch wood with fractal dimension 3 and 1 was 1.0762 mm/min and 0.8559 mm/min, respectively. The basic charring rate of Larch wood with fractal dimension 3 was higher than that of Larch wood with fractal

dimension 1 by 25.74%. The basic charring rate of poplar was 1.1251 mm/min, which was 18.43% higher than that of modern poplar, 60.73% higher than the recommended value in the European EC5 standard, 32.54% higher than the calculated value in the Australian code, and 26.42% higher than the calculated value in the American AFPA.

4. Conclusions

The following results were obtained from a study of five types of ancient wood from six traditional buildings demolished for maintenance:

- (1) The ignition time of ancient wood is earlier than that of modern wood of the same species. The ignition time of softwood is earlier than that of hardwood, with poplar having the shortest ignition time of 7 s and Larch wood 11 s. The ignition time of hardwood is mostly above 15 s, among which the ignition time of Ailanthus wood is the longest at 30 s. The peak burning time of all five kinds of ancient wood is higher than that of modern wood, with the peak burning time of Larch wood is the highest, reaching $149.21 \text{ kw}\cdot\text{m}^{-2}$, and its average burning calorific value was also the highest at $72.07 \text{ kw}\cdot\text{m}^{-2}$.
- (2) There are also differences in the combustion characteristics of ancient wood with different fractal dimension classes on the surface. The ignition times of grade 1 specimens with fractal dimension below 1.4 were mostly longer than those of wood with fractal dimension above 1.4. The more complex the surface morphology, the earlier the ignition time. The highest heat release peaks were mostly for fractal dimension class 3, and the peak heat release of Ulm wood A3 reached $166.84 \text{ kw}\cdot\text{m}^{-2}$ at 35 s, which was nearly $40 \text{ kw}\cdot\text{m}^{-2}$ higher than the highest value for the same species with fractal dimension class 1, and 15 s earlier, with high surface deterioration and large contact area between the outermost layer and oxygen, and the heat release rate peaks earlier. For the same fractal dimension class, the appropriate total amount per unit time is higher for softwood than for hardwood. The higher the fractal dimension class, the higher the basic charring rate.
- (3) The burning characteristics of ancient wood are very different from those of modern wood due to its own special characteristics of natural degradation over hundreds of years. Ancient wood ignites earlier than modern wood of the same species. The heat release rate curves of Larch wood and Salix wood did not show a smooth trend after the first peak after a decline, showing irregular changes. This is mainly due to the premature failure of their charred layers and poor heat resistance. Most of the basic charring rates of traditional buildings were significantly higher than those of modern wood, and the basic charring rates of traditional buildings with surface fractal dimension class 1 were on average in the range of 0.5–2.0 mm/min, most of which were higher than the recommended and calculated values in the standard. Compared to modern wood, ancient wood burning makes the fire more difficult to control. Overall, the differences in combustion characteristics between ancient and modern wood, the earlier ignition time and the irregularity of the heat release rate curve greatly increase fire risk and require extra attention in terms of fire protection.

In this study, due to the use of ancient wood dismantled after the restoration of traditional buildings as the test material, the material is very precious. The number of repeated experiments is limited and there are not many experimental data. It is hoped that the data from this study can help the field of traditional building fire prevention to establish a more accurate model for fire prediction. The data related to the combustion characteristics of ancient wood are used in the data import of the fire model to replace modern wood and better fit the real fire scenario. This provides more reasonable suggestions in the follow-up of fire safety and provides a basis for the assessment of building fire hazard and fire safety level.

Author Contributions: Y.W. wrote the original draft of the manuscript and performed most of the numerical analysis work and experiments. W.W. provided all the experimental materials and put forward guiding opinion in the experiment. H.Z. supervised the research team and provided some ideas for research as well as revised the manuscript. F.Q. provided technical suggestions for the research. All authors have read and agreed to the published version of the manuscript.

Funding: This project was supported by research funding from the Cultural Relics Science and Technology Project of Shanxi Province.

Institutional Review Board Statement: Not applicable.

Informed Consent Statement: Not applicable.

Data Availability Statement: All data used during the study appear in the submitted article.

Conflicts of Interest: The authors declare no conflict of interest.

References

1. Praticò, Y.; Ochsendorf, J.; Holzer, S.; Flatt, R. Post-fire restoration of historic buildings and implications for Notre-Dame de Paris. *Nat. Mater.* **2020**, *19*, 817–820. [CrossRef]
2. Friquin, K. Material properties and external factors influencing the charring rate of solid wood and glue-laminated timber. *Fire Mater.* **2010**, *35*, 303–327. [CrossRef]
3. Ji, J.; Sun, J.; Zhang, Y.; Li, J. Study on surface fire spread characteristics of carbonizable solid combustible materials in alpine environment. *Chin. Sci. Bull.* **2009**, *54*, 1127–1132.
4. Beaumont, O.; Schwob, Y. Influence of physical and chemical parameters on wood pyrolysis. *Ind. Eng. Chem. Process. Des. Dev.* **1984**, *23*, 637–641. [CrossRef]
5. Kanury, A.; Blackshear, P. Some Considerations Pertaining to the Problem of Wood-Burning. *Combust. Sci. Technol.* **1970**, *1*, 339–356. [CrossRef]
6. Maraveas, C.; Miamis, K.; Matthaiou, C. Performance of Timber Connections Exposed to Fire: A Review. *Fire Technol.* **2013**, *51*, 1401–1432. [CrossRef]
7. Tomassetti, M.; Campanella, L.; Tomellini, R. Thermogravimetric analysis of ancient and fresh woods. *Thermochim. Acta* **1990**, *170*, 51–65. [CrossRef]
8. Daouk, E.; Van de Steene, L.; Paviet, F.; Salvador, S. Thick wood particle pyrolysis in an oxidative atmosphere. *Chem. Eng. Sci.* **2015**, *126*, 608–615. [CrossRef]
9. Weng, W.; Hasemi, Y. A numerical model for flame spread along combustible flat solid with charring material with experimental validation of ceiling flame spread and upward flame spread. *Fire Mater.* **2008**, *32*, 87–102. [CrossRef]
10. Janssens, M. A Thermal Model for Piloted Ignition of Wood Including Variable Thermophysical Properties. *Fire Saf. Sci.* **1991**, *3*, 167–176. [CrossRef]
11. Li, Y. Determination of Wood Ignition Temperature. *Fire Sci.* **1992**, *1*, 25–30. Available online: <https://kns.cnki.net/kcms/detail/detail.aspx?FileName=HZKX199201005&DbName=CJFQ1992> (accessed on 20 December 2021).
12. Ji, J.; Cheng, Y.; Yang, L.; Guo, Z.; Fan, W. Experimental study of wood ignition under variable heat flow conditions. *Combust. Sci. Technol.* **2005**, *11*, 448–453.
13. Zhang, X.; Zhang, F. Study on the Pyrolysis Kinetics Characteristics of the Wood from the Ancient Buildings. *Adv. Mater. Res.* **2012**, *568*, 13–16. [CrossRef]
14. Yin, Y.; Luo, B.; Zhang, Z.; Zhang, X.; Cheng, Y.; Jiang, X. Introduction to the application of non-destructive testing methods in wood structure ancient architecture. *Anc. Archit. Gard. Technol.* **2010**, *3*, 20–23.
15. Frangi, A.; Fontana, M. Fire safety of multistorey timber buildings. *Proc. Inst. Civ. Eng. Struct. Build.* **2010**, *163*, 213–226. [CrossRef]
16. Frangi, A.; Fontana, M. Charring rates and temperature profiles of wood sections. *Fire Mater.* **2003**, *27*, 91–102. [CrossRef]
17. Frangi, A.; Erchinger, C.; Fontana, M. Charring model for timber frame floor assemblies with void cavities. *Fire Saf. J.* **2008**, *43*, 551–564. [CrossRef]
18. Frangi, A.; Fontana, M.; Mischler, A. Shear behaviour of bond lines in glued laminated timber beams at high temperatures. *Wood Sci. Technol.* **2004**, *38*, 119–126. [CrossRef]
19. Frangi, A.; Knobloch, M.; Fontana, M. Fire design of timber slabs made of hollow core elements. *Eng. Struct.* **2009**, *31*, 150–157. [CrossRef]
20. Bai, Z. Research on Fire Prevention and Renovation Techniques for Wood Structure Ancient Buildings. Ph.D. Thesis, Shenyang University of Architecture, Shenyang, China, 2017.
21. Gao, X. Study on the Spread of Fire in Wood-Frame Dwellings in Yunnan Province. Ph.D. Thesis, Kunming University of Technology, Kunming, China, 2015.
22. Hong, T.; Park, S.H. FDS Simulation of PMMA Combustion Experiments Performed using ISO 5660 Cone Calorimetry. *J. Adv. Eng. Technol.* **2017**, *10*, 147–152. [CrossRef]

23. Schmid, J.; Klippel, M.; Just, A.; Frangi, A. Review and analysis of fire resistance tests of timber members in bending, tension and compression with respect to the Reduced Cross-Section Method. *Fire Saf. J.* **2014**, *68*, 81–99. [[CrossRef](#)]
24. Steer, P. EN1995 Eurocode 5: Design of timber structures. *Proc. Inst. Civ. Eng. Civ. Eng.* **2001**, *144*, 39–43. [[CrossRef](#)]
25. Canadian Commission on Building and Fire Codes; National Research Council of Canada. *National Building Code of Canada*; National Research Council Canada: Ottawa, Canada, 2015.
26. ANSI Webstore. Timber Structures-Fire Resistance for Structural Adequacy of Timber Members (FOREIGN STANDARD). 2021. Available online: <https://webstore.ansi.org/Standards/SAI/17202006-1159369> (accessed on 20 December 2021).
27. Wen, L. Study on the Burning Charring Behavior of six Commonly Used Tree Species in China. Ph.D. Thesis, China Academy of Forestry Science, Beijing, China, 2016.
28. Liu, L. Study on the Pyrolytic Properties of Silver Middle Poplar and Larch. Ph.D. Thesis, Shenyang Agricultural University, Shenyang, China, 2018.
29. Chen, Z.; Xu, L. Research on fire protection design method for beam and column wood members based on charring rate. *J. Civ. Eng.* **2018**, *51*, 11–20.
30. Wang, X.; Zhang, S. A review on the analysis of wood charring rate and its influencing factors. *Struct. Eng.* **2018**, *34*, 177–182.